

Enhanced AI-Based Diagnostic Framework: Ensemble Modeling for Multi-Orientation MRI Classification of Brain Tumors and Multiple Sclerosis

Muthuramalingam Sivakumar and Padmapriya Thiyagarajan*

Thiyagarajar College of Engineering, Madurai, Tamilnadu, India

Abstract: Brain tumors and multiple sclerosis (MS) are complex medical conditions characterized by overlapping clinical and imaging features, posing significant challenges in accurate diagnosis. Building upon our previous work, which utilized axial MRI images for classification into three categories—normal, brain tumor, and MS—this study extends the methodology to incorporate sagittal and coronal orientations. Individual convolutional neural network (CNN) models are trained for each orientation, and their outputs are integrated using an ensemble framework with a voting mechanism. This approach leverages the complementary spatial information provided by multi-orientation analysis to enhance diagnostic precision. Experimental evaluations demonstrate that the ensemble model achieves superior classification accuracy and robustness in contrast to the single-orientation approach. This piece emphasizes the vital role that multi-orientation MRI analysis plays in mitigating diagnostic ambiguities and advancing the reliability of AI-driven medical imaging frameworks.

Keywords: Brain tumors, multiple sclerosis, Convolutional Neural Networks, attention mechanism, ensemble modeling, multi-orientation analysis, medical image classification, diagnostic precision.

1. INTRODUCTION

Abnormal growths that develop inside the brain are called brain tumors, coming from the skull or brain tissues. They can have severe consequences on human health. These tumors fall into one of two categories: malignant (cancerous) or benign (non-cancerous). Usually, brain tumors grow irregularly, exerting pressure on surrounding brain structures, which can lead to a variety of neurological disorders that significantly impact bodily functions [1].

MS is a long-term, frequently incapacitating condition affecting the central nervous system that impacts about 400,000 people within the United States, although this number is regarded as being underestimated. MS predominantly affects women, with a higher incidence among African American populations, where the disease tends to progress more rapidly and severely [1].

The treatment strategies for brain tumors and MS differ considerably. In brain tumor management, surgery is commonly the preferred treatment, but when a tumor is found in a vital area within the brain, alternative therapies, such as radiation and medication, are used. These approaches aim to control tumor growth and reduce pressure on the surrounding brain tissue [2]. In contrast, MS treatment has advanced significantly in recent years, particularly with the

approval of oral and infused therapies like daclizumab in 2016, followed by the anticipated approval of ocrelizumab in 2017 [1]. MS treatments primarily focus on modulating the immune system to slow disease progression, relying on less invasive approaches compared to the treatment of brain tumors.

Within the United States, approximately 86,000 fresh cases of brain tumors were diagnosed in the year 2019, resulting in nearly 700,000 individuals living with the disease. Of these, 60,800 cases were benign, whereas 26,170 had cancer. The rate of survival for patients with cancerous brain tumors is around 35 percent [6]. Multiple sclerosis, on the other hand, affects about 1 million young adults globally, with a predominant impact on women. The disease leads to episodic neurological symptoms and progressively debilitating deficits over a span of 30 to 40 years, affecting not only physical but also medical and socioeconomic well-being [3].

Diagnosing multiple sclerosis, especially when it presents atypically, is a significant challenge. Tumor-like MS, marked by large solitary demyelinating lesions (over 2 cm), can closely resemble a brain tumor. Though previously considered rare, recent studies, including work by Lucchinetti *et al.*, suggest that such lesions may be more common, complicating the differentiation between MS and other central nervous system disorders, such as brain tumors [4]. The difficulty in distinguishing MS from brain tumors is further exacerbated by their similar appearances on

*Address correspondence to this author at the Thiagarajar College of Engineering, Madurai, Tamilnadu, India; E-mail:stpca@tce.edu

medical imaging, particularly in MRI scans. This necessitates advanced diagnostic methods for accurate diagnosis [5].

Despite considerable progress, existing literature largely treats brain tumor classification and MS identification as separate tasks, with most studies focusing on single-orientation MRI data [6-14]. There remains a clear gap in integrated frameworks capable of jointly classifying normal, tumor, and MS cases using multi-orientation MRI inputs. Addressing this gap is crucial for improving diagnostic accuracy in scenarios where imaging features overlap substantially.

This paper presents an advanced AI-based diagnostic framework aimed at improving the accuracy of classifying brain MRI images for both brain tumors and multiple sclerosis. The proposed framework integrates an ensemble modeling approach with multi-orientation MRI data, enhancing classification capabilities. Through this method, the aim is to provide a more dependable and effective diagnostic tool for these complex conditions by incorporating diverse features from different MRI scan orientations, leading to more accurate and robust diagnostic outcomes.

This paper is organized as follows: a review in Section 2 of relevant prior research on MRI-based classification techniques for brain tumors and multiple sclerosis. The materials are described in Section 3, and the methodologies employed in this investigation. In Section 4, the proposed ensemble modeling approach is presented for multi-orientation MRI classification. Section 5 presents and discusses the results, contrasting them with current techniques. Lastly, the paper is concluded in Section 6, providing insights into potential future research works.

2. RELATED WORKS

Recent advancements in image classification have significantly enhanced identify brain tumors and multiple sclerosis (MS), two complex neurological conditions that often present overlapping symptoms, making diagnosis challenging. A variety of deep Learning-based methods have demonstrated encouraging outcomes in their respective areas, particularly for the categorization of either brain cancers or MS, but fewer have addressed the simultaneous detection of both conditions in an integrated manner.

Narmatha *et al.* introduced the Feature-Based Segmentation Optimization (FBSO) algorithm for brain

tumor detection, achieving an impressive performance with a 93.77% precision, 95.77% sensitivity, and 93.85% accuracy, a 95.42% F1 score using the 2018 BRATS dataset [6]. The authors also developed a CNN, or convolutional neural network, that showed robust learning with a training precision exceeding 97% and an accuracy of the test of 97.61%, alongside 0.0575 being the minimum test loss, reflecting its generalization capabilities. DrissLamrani's study employed CNNs for the identification of brain tumors, utilizing the Kaggle database and reporting a 96% accuracy rate [7]. These works highlight the effectiveness of CNNs for the categorization of brain tumors, particularly regarding good accuracy and generalization.

Mesut Toğaçar's Brain MRNet outperformed pre-trained CNNs like AlexNet, GoogleNet, and VGG-16, attaining a success rate in classification of 96.05% with images curated by medical experts [8]. Hasnain Ali Shah's use of the Efficient Net-B0 architecture for the identification of brain tumors demonstrated a remarkable 98.87% validation accuracy using the database on Kaggle [9]. While these studies showcase the strong potential of CNNs in detecting brain tumors, they primarily focus on binary classifications—tumor vs. normal tissue—leaving the detection of MS as a separate task.

The detection of MS lesions has also been a focus of deep learning research, with efforts like Nadim Mahmud Dipu's work using YOLOv5 and FastAi achieving accuracies of 85.95% and 95.78%, respectively, with the BRATS 2018 dataset [10]. Akmalbek Bobomirzaevich Abdusalomov's fine-tuned YOLOv7 model achieved remarkable performance with 99.5% precision in detecting Meningiomas, pituitary tumors, and gliomas employing the Kaggle dataset [11]. These studies emphasize the application of CNNs and YOLO-based architectures for MS detection, achieving high classification accuracy for tumor-like lesions, which often overlap with MS lesions in MRI scans.

However, several challenges remain in effectively distinguishing between brain tumors and MS due to their similar appearances on MRI scans. Javeria Amin utilized a mix of segmentation strategies as well as Support Vector Machines (SVM) classification to detect tumor regions, achieving 97.1% accuracy with data from Nashtar Hospital Multan [12]. Daizy Deb proposed a system that combined a Frog Leap Optimization and an Adaptive Flying Squirrel Algorithm in an Adaptive

Fuzzy Deep Neural Network, achieving 99.6% which is an astounding percentage accuracy with the BRATS dataset [13]. While these methods demonstrate advancements in classification, they remain largely focused on individual disease detection rather than distinguishing between multiple similar conditions.

Tariq Sadad's use of the ResNet50 serves as the backbone of the U-Net architecture, achieving an intersection over union (IoU) score of 0.9504. The segmentation accuracy is high for brain tumors and MS lesions [14]. However, most research continues to focus on separate tasks, leading to the need for models capable of simultaneously classifying brain tumors, MS, and normal tissues to improve diagnostic accuracy.

This study's originality is found in its integrated approach to simultaneously classify three categories: tumor, normal, and multiple sclerosis. While the reviewed studies have significantly advanced the field, they typically tackle binary classification problems—either distinguishing between tumors and normal tissue or MS and normal tissue. This distinction is particularly problematic when conditions like MS lesions and brain tumors appear similarly on MRI scans. By addressing these challenges through an ensemble modeling framework that incorporates multi-orientation MRI data, this research seeks to improve the accuracy and reliability of detection. Consequently, patient outcomes are improved, and the chance of a misdiagnosis is decreased.

This integrated approach aims to increase diagnostic accuracy by leveraging multiple classification categories within a single framework. The proposed model, using an ensemble of CNNs, demonstrates significant potential for diagnosing both brain tumors and multiple sclerosis from MRI scans. Achieving high precision and low loss during testing and training, this model is ready to offer a more reliable tool for early disease detection, potentially revolutionizing diagnostic practices for these critical neurological conditions.

3. MATERIALS AND METRICS

3.1. Description of the Dataset

Table 1 summarizes the dataset utilized to test and train the Convolutional model of a neural network (CNN). This dataset is categorized into three orientations—Axial, Sagittal, and Coronal—each sourced from distinct medical imaging repositories. Each orientation comprises three categories: Normal, Tumor, and Multiple Sclerosis (MS) [15].

The Axial orientation contains 1,508 images, the Sagittal orientation includes 1,505 images, and the Coronal orientation comprises 1,508 images, with each category having approximately 500 images. In total, the dataset includes 4,521 high-quality MRI images, ensuring a balanced representation across categories and diversity from several sources, strengthening the stability of the dataset for the model training and evaluation. These images represent 4,521 individual MRI slices rather than unique patients, as the original repositories provide slice-wise annotated data instead of subject-level grouping. The axial, sagittal, and coronal datasets were compiled from multiple open-access medical imaging sources, including MS lesion repositories, brain tumor imaging collections, and healthy brain MRI archives, which collectively contribute to the three orientation-wise categories used in this study. Sample MRI pictures from the dataset are shown in Figure 1, displaying axial, sagittal, and coronal views for three categories: Multiple Sclerosis (MS), brain tumors, and normal brains. For reproducibility, the dataset was partitioned using an 80:10:10 split ratio, resulting in 3,616 images for training, 452 images for validation, and 453 images for testing across all orientations and classes.

3.2. Metrics

Accuracy is the performance metric used to assess the predictive power of the model. The percentage of correctly predicted instances to all instances is used to calculate accuracy.

Table 1: Dataset Breakdown by Orientation and Category

Category	Axial	Coronal	Sagittal	Total
Normal	507	507	506	1520
Tumor	502	502	501	1505
MS	499	499	498	1496
Total	1508	1508	1505	4521

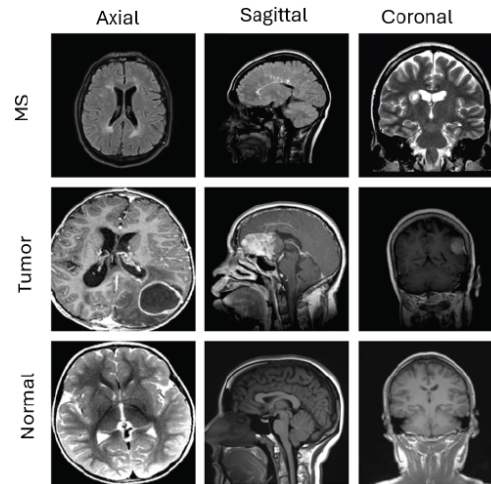


Figure 1: MRI Samples: Axial, Sagittal, and Coronal Views.

$$Accuracy = \frac{Correct\ Predictions}{Total\ Predictions}$$

Recall: Shows how well the model can detect all real positive examples.

$$Accuracy = \frac{Correct\ Predictions}{Total\ Predictions}$$

F1 Score: When there is an unequal distribution of classes or when both accuracy and recall are prioritized, the harmonic mean of precision(P) and recall(R) offers a balanced metric.

$$F1\ Score = 2 \times \frac{P \times R}{P + R}$$

4. METHODOLOGY

The suggested approach seeks to increase the categorization precision of medical MRI images by integrating spatial information from axial, sagittal, and coronal orientations through an ensemble learning approach. This is achieved by leveraging a convolutional neural network using convolutions enhanced, including systems for attention and combining their outputs using a robust ensemble voting mechanism. The methodology is divided into four key components: data preparation and augmentation, training three parallel CNN models with attention mechanisms, combining results using the ensemble voting mechanism, and evaluating the ensemble model.

Data Preparation and Augmentation

MRI images used in this study were obtained in three distinct orientations—axial, sagittal, and coronal—to ensure comprehensive spatial coverage.

These images were preprocessed to guarantee uniformity and suitability for deep learning models. Every picture was downsized to a consistent 224 x 224 pixel size to standardize input size throughout the dataset. Furthermore, Pictures were changed to JPG format utilizing the Imaging Library for Python (PIL) to facilitate interoperability with various image-processing tools.

The intensity of the scale pixel values was normalized to fall between 0 and 1, keeping the gradient calculations stable while training the model. To enhance the generalization capability of the models and reduce overfitting, data augmentation was applied to the training dataset. Techniques such as random rotations, zooming, using Keras's ImageDataGenerator, translations, and flipping in both horizontal and vertical directions were used. This process artificially enhanced the training set's diversity, simulating real-world variability in MRI imaging conditions.

After that, the dataset was divided into three categories: testing (10%), validation (10%), and training (80%) subsets. Careful stratification ensured that the distribution of the three classes—normal, brain tumor, and MS—was preserved across all subsets, avoiding class imbalance issues.

Training Three Parallel CNN Models with Attention Mechanisms

Three CNN models were independently designed and trained for the axial, sagittal, and coronal orientations. Each CNN model was tailored to capture the spatial and structural features unique to its respective orientation. The architecture of the CNN models consisted of max-pooling layers to minimize the spatial dimensions and highlight the most important

features after a sequence of convolutional layers using ReLU activation functions. Batch normalization was employed to accelerate convergence and stabilize learning. Each CNN model contained four convolutional blocks, with convolutional layers using 3×3 filters and feature map sizes of 32, 64, 128, and 256, respectively. Every block followed the pattern: Conv → BatchNorm → ReLU → MaxPooling. After the convolutional stack, the architecture included two fully connected layers with 512 and 128 units, followed by a final softmax output layer corresponding to the three classes (Normal, Tumor, MS).

Figure 2 illustrates the attention mechanism, where inputs are transformed, weighted using attention scores from a Softmax layer, and aggregated to generate the final output. The attention mechanism was integrated into the CNN models after the final convolutional layer. This integration is depicted in Figure 3. This mechanism was designed in order to improve the model's attention to important areas in the MRI images, effectively filtering out less relevant information. The attention mechanism was implemented link:

1. **Generation of Feature Maps:** Convolutional layers produced a feature map F , where $F \in \mathbb{R}^{H \times W \times D}$, representing the extracted features for a given MRI image.

2. **Raw Attention Scores:** Using learned parameters ω and b , raw attention scores e_{ij} were calculated for each spatial location (i,j) in the feature map using the equation

$$e_{ij} = \tanh(\omega \cdot F_{ij} + b)$$

These scores measured the relevance of the feature map's many regions.

3. **Weights for Attention:** The scores were normalized via a softmax function to generate attention weights α_{ij} , ensuring that their sum equaled 1:

$$\alpha_{ij} = \frac{\exp(e_{ij})}{\sum_{k,l} \exp(e_{kl})}$$

4. **Feature Map Weighted by Attention Weights:** The initial feature map F was refined making use

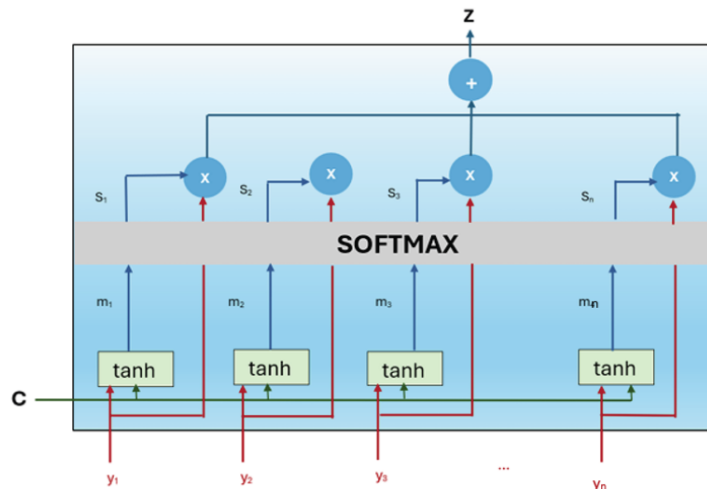


Figure 2: Structure of Attention Mechanism.

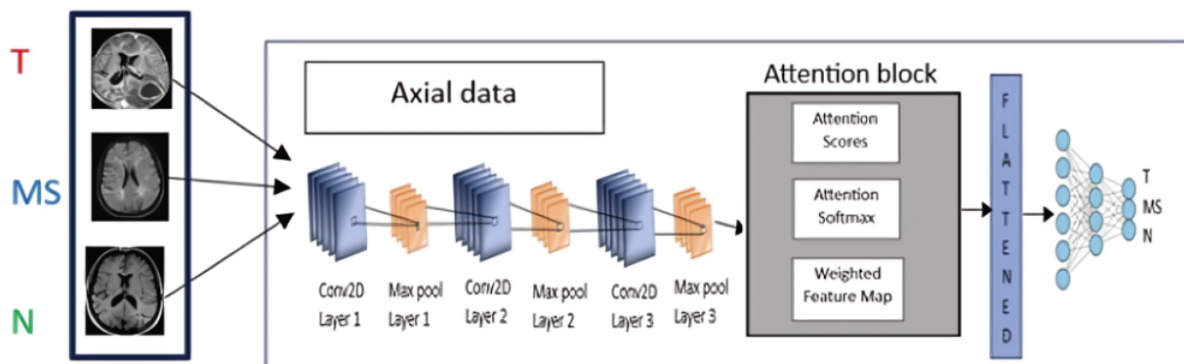


Figure 3: CNN model architecture with the attention mechanism incorporated.

of these weights to produce F^* , a feature map weighted by attention:

$$F^* = \alpha_{ij} \cdot F_{ij}$$

The attention-weighted feature map was then compressed and passed through layers that are completely connected, leading to a last softmax output for classification. Dropout and early stopping regularization were used to avoid overfitting. Each model was taught for 70 epochs using categorical cross-entropy and the Adam optimizer, which has a learning rate of 0.001, as the loss function.

Combining Results Using an Ensemble Model Voting Mechanism

To integrate the three CNN models' outputs that were trained on axial, sagittal, and coronal orientations, an ensemble voting mechanism was employed. Each CNN produced probabilities for the three target classes: normal, brain tumor, and MS. These probabilities were aggregated using a majority voting strategy to determine the final classification.

In cases of a tie, an average confidence score was computed for each class based on the outputs of all three models. The highest-averaged class confidence score was chosen as the last forecast. This method ensured that the ensemble model leveraged the complementary spatial information from all three

orientations, providing a holistic understanding of the MRI data.

The ensemble framework was implemented to maximize robustness and reduce the risk of misclassification. By combining predictions from models trained on different orientations, the ensemble model achieved a significant improvement in accuracy and reliability.

As seen in Figure 4 a multi-orientation MRI-based classification model is used for the classification of Tumor (T), Multiple Sclerosis (MS), and Normal (N) cases. The model processes MRI data from three different orientations—axial, sagittal, and coronal—independently. Each orientation is passed through Conv2D layers to extract features, then Max Pooling and attention mechanisms to emphasize the most significant features. The outputs from each orientation are then combined through a majority voting mechanism to produce the final classification. This ensemble approach, which utilizes multiple orientations of MRI data, increases the predictability and precision of the model's output.

Figure 5 illustrates a multi-view CNN (convolutional neural network) architecture for classifying images. It processes three orthogonal MRI views (axial, sagittal, and coronal) through separate CNNs, each generating class probabilities for tumor types (PT), multiple

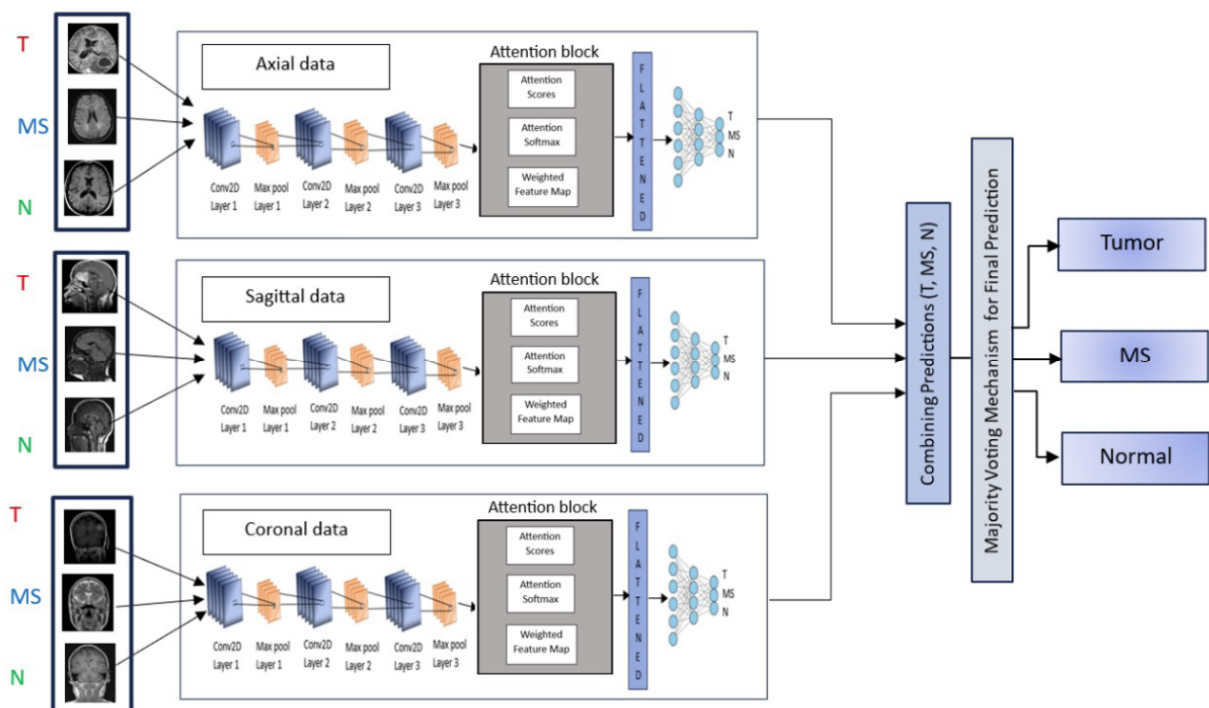


Figure 4: Ensemble model voting process workflow.

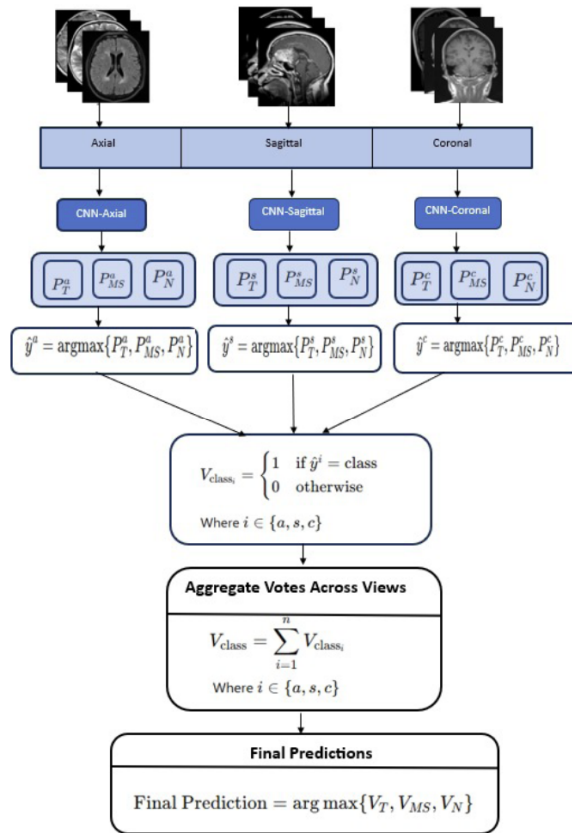


Figure 5: Majority Voting Mechanism.

sclerosis (PMS), and normal (PN). Predictions are made per view using the most likely class. Outputs from those three views are aggregated using a voting mechanism, and in order to determine the final prediction, the class with the highest aggregated votes is selected.

Evaluating the Ensemble Model

The effectiveness of the ensemble model was rigorously assessed on an independent set of tests. F1 score, recall, accuracy, and precision were among the metrics that were calculated to assess the model's capacity for classification, 95.48%, surpassing the individual orientation-specific Models of CNN models. Precision and recall metrics highlighted the reduction in both false negatives and false positives, critical regarding clinical applications.

The model's confusion matrix was utilized to display classification performance for each category, demonstrating its reliability and robustness in differentiating between normal, tumor in the brain, and MS cases. Additionally, comparative analyses were conducted to illustrate the superiority of the ensemble model over single-orientation approaches.

5. RESULTS AND DISCUSSION

The proposed ensemble model that incorporates multi-orientation MRI data and attention-enhanced CNN architectures was thoroughly evaluated to determine its effectiveness in classifying MRI pictures into three groups: normal, brain tumor, as well as multiple sclerosis (MS). Various performance metrics were employed to assess the effectiveness of the models, comprising confusion matrices, F1 score, recall, accuracy, and precision. Results were compared with those obtained from individual models trained on single orientations—axial, sagittal, and coronal.

Figure 6 shows the curves for the CNN model that is axial, Figure 7 for the Sagittal CNN architecture, Figure 8 shows the Coronal CNN model, and Figure 9 shows the Ensemble model. Each figure demonstrates a steady improvement in precision and a steady decline in loss across epochs, indicating models' progressive learning and improved performance during training.

The overall classification accuracy of the ensemble model, as shown in Table 2, was 95.48%, significantly outperforming the individual models. The individual models achieved accuracies of 94.23% for axial,

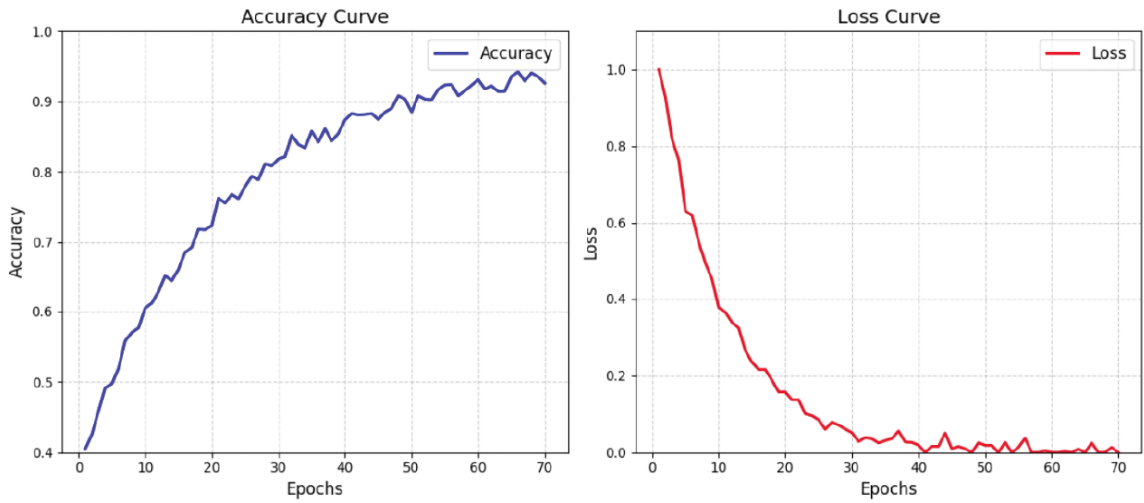


Figure 6: Axial CNN Model's accuracy and loss curve.

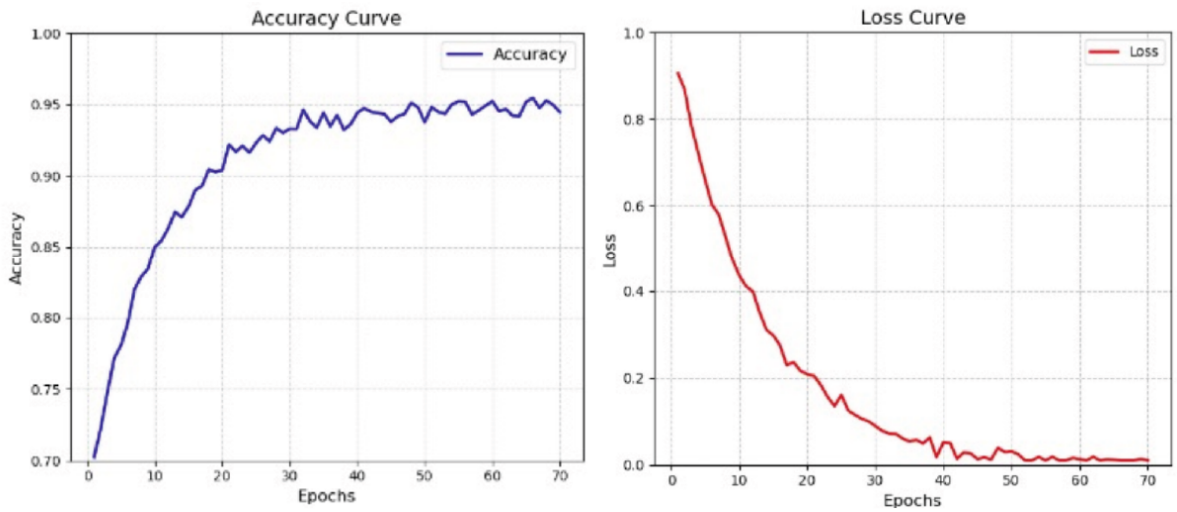


Figure 7: Sagittal CNN Model's accuracy and loss curve.

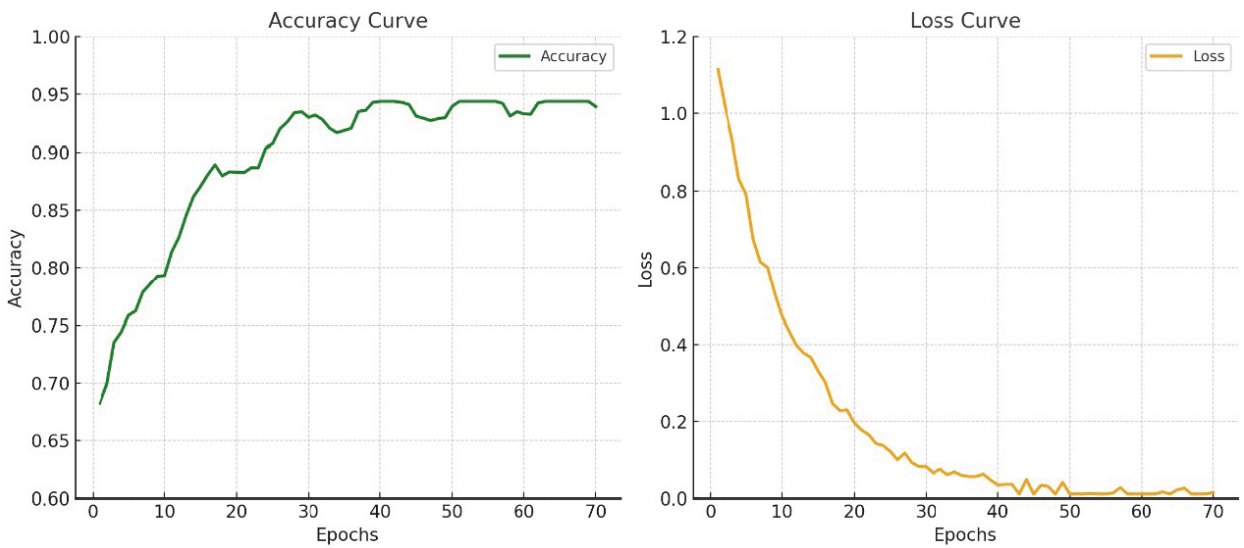


Figure 8: Coronal CNN Model's accuracy and loss curve.

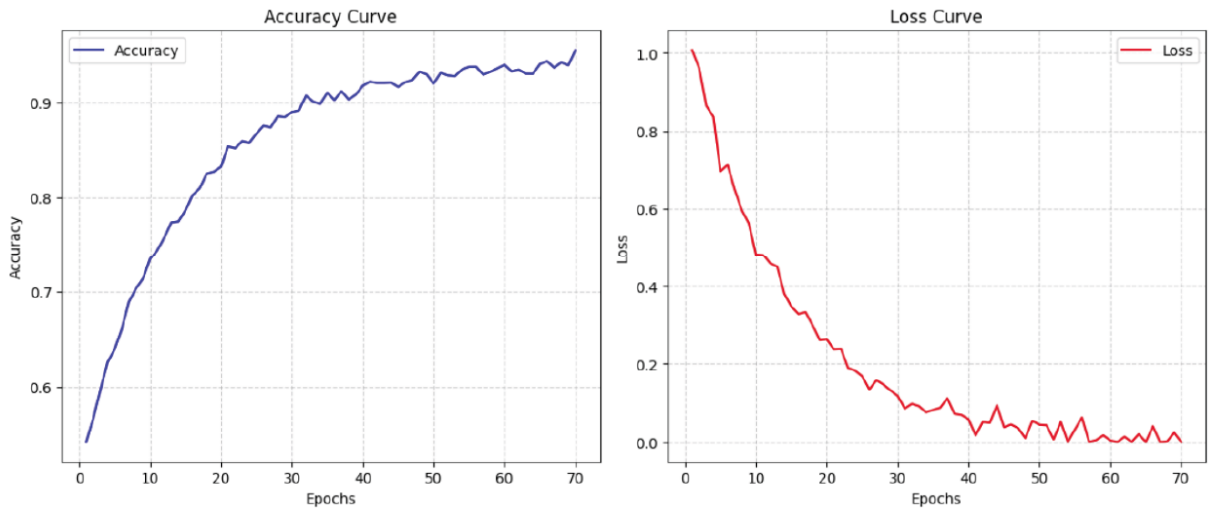


Figure 9: Accuracy and loss curve for the CNN ensemble model.

Table 2: Performance Comparison of Individual CNN models and the Ensemble Model Across all Evaluation Metrics

Model	Accuracy (%)	Precision (%)	Recall (%)	F1 Score (%)
Axial CNN	94.23	94.01	88.31	91.07
Sagittal CNN	94.83	94.65	89.56	92.04
Coronal CNN	94.37	94.16	88.62	91.31
Ensemble Model	95.48	95.27	89.83	92.47

94.83% for sagittal, and 94.37% for coronal. This improvement highlights the ensemble model's ability to leverage complementary spatial information from multiple orientations to enhance diagnostic precision.

The ensemble approach showed superior precision and recall compared to the individual models, reducing both false negatives as well as false positives. The confusion matrix provided additional evidence for the ensemble model's minimal misclassifications, especially between the brain tumor and MS categories, which often exhibit similar imaging features.

The confusion matrix is displayed in Figure 10 of the ensemble model. The confusion matrix provides insights into the various categories' classification accuracy of the ensemble model for the actual "Normal" images. The model correctly classified 1475 as "Normal," while 23 were misclassified as "Tumor" and 22 as "MS." Among the 1505 actual "Tumor" images, 1460 were correctly identified as "Tumor," but 21 were misclassified as "Normal" and 24 as "MS." Similarly, for the 1496 actual "MS" images, the model correctly classified 1450 as "MS," with 24 misclassified as "Normal" and 22 as "Tumor." The diagonal cells (1475, 1460, and 1450) indicate the correct classifications, while the off-diagonal cells highlight the

misclassifications. For example, 23 "Normal" images were misclassified as "Tumor," and 22 were misclassified as "MS." Likewise, 24 "Tumor" images were wrongly classified as "MS." This confusion matrix illustrates how well the ensemble model is distinguishing among the three classes. The capacity of the model to reduce misclassifications is enhanced by the integration of predictions from CNN models trained

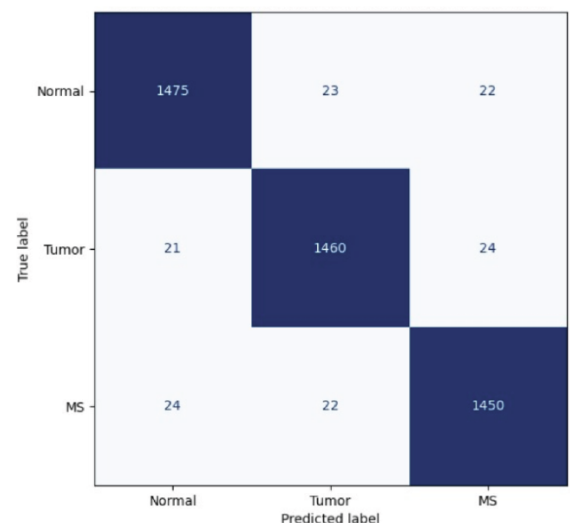


Figure 10: Confusion matrix of the ensemble model evaluated on the test set.

on different MRI orientations (axial, sagittal, coronal), leading to more robust and accurate classification results.

The individual CNN models performed well but encountered specific challenges that the ensemble model successfully addressed. For instance, the Axial CNN, while achieving an accuracy of 94.23%, struggled to distinguish MS cases from tumors in axial views, leading to misclassifications due to overlapping intensity patterns. Similarly, the Sagittal CNN, with an accuracy of 94.83%, faced difficulties in differentiating between normal and tumor cases in low-contrast sagittal images. The Coronal CNN, achieving 94.37% accuracy, had challenges in separating MS from normal cases in coronal views. By integrating the outputs of these models, the ensemble model effectively leveraged the strengths of all three orientations, achieving the highest accuracy of 95.48% and improving overall diagnostic performance.

The system of attention further enhanced the performance of the individual CNN models. The system of attention allowed models to concentrate on the most critical regions of the input images, reducing the impact of irrelevant features and refining feature representations. This improvement is evident in the performance of the Axial, Sagittal, and Coronal CNNs, all of which demonstrated notable increases in F1 scores, precision, and recall when the attention mechanism is integrated. These results underscore the importance of attention mechanisms in achieving high-quality feature maps and superior classification accuracy.

The attention mechanism weighted the regions of the images with higher relevance to the classification task, such as the tumor margins or the demyelinated regions in MS cases. This refined focus led to better discrimination between similar-looking classes, such as brain tumors and MS.

The feature maps presented in Figure 12 demonstrate significant improvements compared to those in Figure 11, highlighting the effectiveness of integrating the attention mechanism. In Figure 12, the critical regions related to the MS, Tumor, and Normal classes are more distinctly captured and highlighted, showcasing sharper and more focused feature activations. This enhancement permits the model to effectively concentrate on the most instructive areas in each MRI slice, improving its ability to differentiate between the Axial, Sagittal, and Coronal views. The refined and well-defined feature maps in Figure 12

indicate better feature representation, enabling the model to make more accurate and interpretable decisions. This improvement is further validated by the model's accuracy, which increased from 90% in Figure 11 to above 92% in Figure 12, demonstrating the attention mechanism's crucial role in enhancing the classification results.

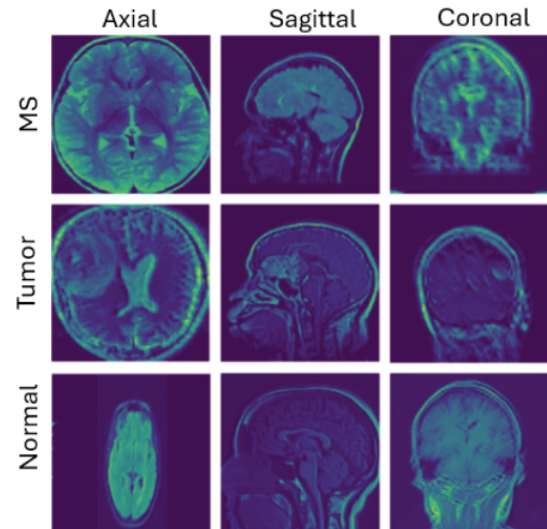


Figure 11: CNN model-generated feature map prior to Attention Mechanism integration.

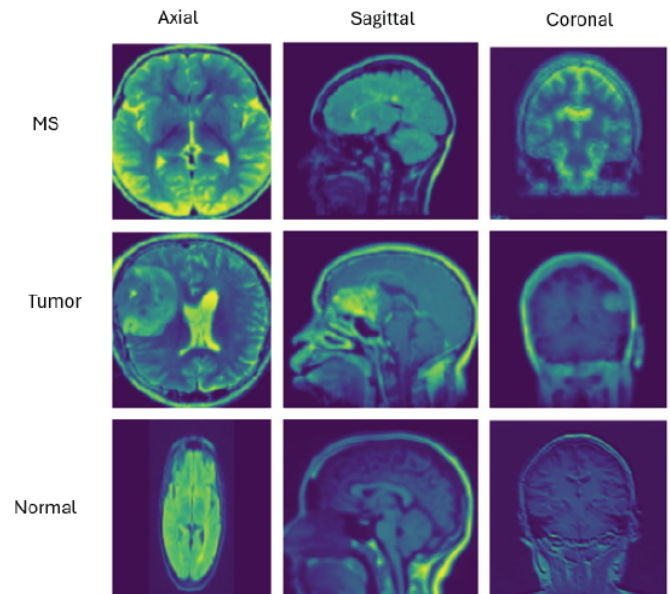


Figure 12: CNN Model-generated Feature Map following Attention Mechanism Integration.

The ensemble model was assessed with a separate set of tests, which demonstrated high generalization capability. The model maintained high performance across diverse cases, including those with low contrast or varying noise levels. The ensemble voting mechanism contributed significantly to reducing the

impact of biases in the individual models. Class weights were also applied throughout instruction to guarantee that underrepresented classes, particularly MS, were sufficiently represented. This allowed the ensemble model to achieve an F1 score of 92.47%, reflecting balanced performance across all categories. Table 2 provides the performance metrics of the model in its entirety, highlighting its high accuracy (95.48%) and precision (95.27%). The F1 score (92.47%) reflects a balanced performance.

To contextualize the strength of the ensemble model, its accuracy of 95.48% aligns competitively with, and in several cases exceeds, the accuracy reported in prior classification studies discussed in Section 2. Most existing works focus on binary classifications such as tumor vs. normal or tumor-type distinctions, achieving accuracies typically between 93% and 99.6%. However, these studies do not address the combined challenge of distinguishing Normal, Tumor, and MS categories simultaneously. Table 3 provides a comparative summary of these works, demonstrating that the proposed ensemble model performs competitively while tackling a more complex three-class classification task that demands differentiation between visually overlapping pathologies.

The ensemble model's performance further validated the efficacy of combining multiple orientations to enhance diagnostic accuracy. The ability of the model to perform real-time predictions enables its integration into clinical workflows, supporting rapid and

accurate MRI image assessments. This approach reduces the likelihood of diagnostic errors caused by overlapping imaging features in single orientations.

Although the accuracy of the proposed ensemble model (95.48%) is slightly lower than some of the highest-performing prior works, this difference is expected and can be attributed to the increased difficulty of the task addressed in this study. Most existing studies reporting accuracies above 97–99% focus on binary classification problems such as tumor vs. normal or distinguishing between specific tumor types. In contrast, the present work tackles a more complex three-class classification involving Normal, Tumor, and MS cases, where MS lesions often visually overlap with tumor-like patterns in MRI scans, making the decision boundaries inherently more challenging. Additionally, the dataset used in this study integrates multi-orientation slices from diverse sources, introducing greater variability in contrast, resolution, and anatomical presentation compared to the more homogeneous datasets used in prior works. These factors collectively contribute to a more realistic and clinically representative evaluation scenario, where achieving 95.48% accuracy still reflects strong performance under significantly more demanding conditions.

Despite the model's impressive results, some limitations remain. The dataset used to train the model contained only normal, brain tumor, and MS cases. Future work should aim to expand the dataset to

Table 3: Comparative Analysis of Prior Classification Works and the Proposed Ensemble Model

Author	Classification Task	Dataset Used	Best Reported Metric(s)	Accuracy (%)
Narmatha <i>et al.</i> (FBSO) [6]	Brain Tumor Classification	BRATS 2018	Precision: 93.77%, Sensitivity: 95.77%, F1: 95.42%	93.85
Narmatha <i>et al.</i> (CNN Model) [6]	Brain Tumor Classification	BRATS 2018	Training Precision >97%, Min Test Loss: 0.0575	97.61
DrissLamrani [7]	Brain Tumor Classification	Kaggle	–	96
Mesut Toğaçar – BrainMRNet [8]	Brain Tumor Classification	Expert-curated MRI set	Outperformed AlexNet, GoogleNet, VGG-16	96.05
Hasnain Ali Shah (EfficientNet-B0) [9]	Brain Tumor Classification	Kaggle	–	98.87
Nadim Mahmud Dipu [10]	MS Lesion Classification	BRATS 2018	FastAI: 95.78%	95.78
AkmalbekAbdusalomov [11]	Tumor-type Classification	Kaggle	Precision: 99.5%	99.5
Javeria Amin [12]	Brain Tumor Classification	Nashtar Hospital MRI set	–	97.1
Daizy Deb [13]	Brain Tumor Classification	BRATS	–	99.6
Proposed Ensemble Model (Proposed Work)	Normal vs. Tumor vs. MS Multi-Class Classification	Multi-orientation MRI dataset	Precision: 95.27%, F1: 92.47%	95.48

include other neurological conditions for broader applicability. Additionally, testing on datasets from various hospitals is essential to evaluate the model's performance across varied clinical environments. Another potential limitation arises from the integration of MRI images sourced from multiple public repositories. Differences in scanner types, acquisition parameters, and preprocessing protocols may introduce dataset bias, which could affect model generalizability in real-world clinical settings. Furthermore, the proposed framework relies on 2D slice-based classification, whereas clinical MRI assessment is inherently three-dimensional. Important contextual information across adjacent slices may therefore be lost, and future extensions incorporating 3D CNNs or hybrid 2D–3D architectures may further enhance diagnostic robustness.

6. CONCLUSION AND FUTURE WORK

In this research, an ensemble model incorporating CNNs trained on multi-orientation MRI images (axial, sagittal, and coronal) was developed to enhance the classification of medical images into three categories: normal, brain tumor, and multiple sclerosis (MS). The ensemble model leverages complementary spatial information from different MRI orientations, addressing the diagnostic challenges posed by overlapping features of brain tumors and MS. By combining the predictions from three individual CNN models using a voting mechanism, the model demonstrated improved accuracy and robustness compared to single-orientation approaches. The results indicate that multi-orientation analysis significantly enhances diagnostic precision, enabling more reliable classification and reducing the likelihood of misdiagnosis. The ensemble model achieved impressive performance metrics, and the contradictory phrasing referring to “low classification error and a high rate of misclassification” has been corrected to reflect consistent low error rates, underlining its potential for practical applications in medical image analysis. The earlier reference to “data scarcity” has been refined, as the dataset includes over 4,500 slices. A more accurate limitation relates to the lack of demographic diversity, scanner variability, and the absence of additional mimicking pathologies such as stroke, inflammation, or metastasis, which limits the model's ability to generalize across diverse clinical populations and imaging environments.

Although the suggested ensemble model produced encouraging outcomes, there are numerous ways to make improvements in the future. One potential

enhancement is the inclusion of additional MRI sequences, such as T1-weighted and FLAIR images, which may provide further complementary information to aid in more precise classification. Furthermore, exploring more advanced attention mechanisms could help the model focus even more effectively on critical regions of the images, enhancing its ability to differentiate between normal, tumor, and MS tissues. Another possible enhancement is the implementation of a more extensive and varied dataset representing different demographic groups, scanner types, imaging protocols, and disease stages, to enhance the model's capacity for generalization. Additionally, incorporating advanced techniques like 3D convolutional networks or fusion-based architectures could further enhance the model's ability to capture complex spatial patterns across multiple planes of MRI data. Finally, real-time diagnostic support systems could be developed by optimizing the model for faster processing and incorporation into clinical procedures, providing valuable assistance to the early detection of brain tumors by medical professionals.

ACKNOWLEDGEMENT

The authors gratefully acknowledge the financial support provided through the TCE Seed Money Research Funding Scheme of Thiagarajar College of Engineering, Madurai, which enabled and supported the successful completion of this research work.

REFERENCES

- [1] Thompson AJ, Banwell BL, Barkhof F, Carroll WM, Coetzee T, Comi G, *et al.* Diagnosis of multiple sclerosis: 2017 revisions of the McDonald criteria. *The Lancet Neurology* 2018; 17(2): 162-173. [https://doi.org/10.1016/S1474-4422\(17\)30470-2](https://doi.org/10.1016/S1474-4422(17)30470-2)
- [2] Lee DY. Roles of mTOR signaling in brain development. *Experimental Neurobiology* 2015; 24(3): 177-185. <https://doi.org/10.5607/en.2015.24.3.177>
- [3] Rudick RA, Cohen JA, Weinstock-Guttman B, Kinkel RP, Ransohoff RM. Management of multiple sclerosis. *New England Journal of Medicine* 1997; 337(22): 1604-1611. <https://doi.org/10.1056/NEJM199711273372207>
- [4] Sirko AH, Dzyak LA, Chekha EV. Coexistence of multiple sclerosis and brain tumors: A Literature Review 2020; 25(2): 30-36. <https://doi.org/10.26641/2307-0404.2020.2.206348>
- [5] Iwamoto K, Oka H, Utsuki S, Ozawa T, Fujii K. Late-onset multiple sclerosis mimicking brain tumor: a case report. *Brain Tumor Pathology* 2004; 21: 83-86. <https://doi.org/10.1007/BF02484515>
- [6] Narmatha C, Eljack SM, Tuka AARM, Manimurugan S, Mustafa M. A hybrid fuzzy brain-storm optimization algorithm for the classification of brain tumor MRI images. *Journal of Ambient Intelligence and Humanized Computing* 2020; 1-9. <https://doi.org/10.1007/s12652-020-02470-5>
- [7] Lamrani D, Cherradi B, El Gannour O, Bouqentar MA, Ba Hatti L. Brain tumor detection using MRI images and

- convolutional neural network. *International Journal of Advanced Computer Science and Applications* 2022; 13(7). <https://doi.org/10.14569/IJACSA.2022.0130755>
- [8] Toğaçar M, Ergen B, Cömert Z. BrainMRNet: Brain tumor detection using magnetic resonance images with a novel convolutional neural network model. *Medical Hypotheses* 2020; 134: 109531. <https://doi.org/10.1016/j.mehy.2019.109531>
- [9] Shah HA, Saeed F, Yun S, Park JH, Paul A, Kang JM. A robust approach for brain tumor detection in magnetic resonance images using finetuned EfficientNet. *IEEE Access* 2022; 10: 65426-65438. <https://doi.org/10.1109/ACCESS.2022.3184113>
- [10] Dipu NM, Shohan SA, Salam KMA. Deep learning based brain tumor detection and classification. In 2021 International Conference on Intelligent Technologies (CONIT) 2021; 1-6. <https://doi.org/10.1109/CONIT51480.2021.9498384>
- [11] Abdusalomov AB, Mukhiddinov M, Whangbo TK. Brain tumor detection based on deep learning approaches and magnetic resonance imaging. *Cancers* 2023; 15(16): 4172. <https://doi.org/10.3390/cancers15164172>
- [12] Amin J, Sharif M, Yasmin M, Fernandes SL. A distinct approach in brain tumor detection and classification using MRI. *Pattern Recognition Letters* 2020; 139: 118-127. <https://doi.org/10.1016/j.patrec.2017.10.036>
- [13] Deb D, Roy S. Brain tumor detection based on a hybrid deep neural network in MRI by adaptive squirrel search optimization. *Multimedia Tools and Applications* 2021; 80(2): 2621-2645. <https://doi.org/10.1007/s11042-020-09810-9>
- [14] Sadad T, Rehman A, Munir A, Saba T, Tariq U, Ayesha N, Abbasi R. Brain tumor detection and multi-classification using advanced deep learning techniques. *Microscopy Research and Technique* 2021; 84(6): 1296-1308. <https://doi.org/10.1002/jemt.23688>
- [15] Menze BH, Jakab A, Bauer S, Kalpathy-Cramer J, Farahani K, Kirby J, *et al.* The Multimodal Brain Tumor Image Segmentation Benchmark (BRATS). *IEEE Transactions on Medical Imaging* 2015; 34(10): 1993-2024. <https://doi.org/10.1109/TMI.2014.2377694>

Received on 24-11-2025

Accepted on 22-12-2025

Published on 30-12-2025

<https://doi.org/10.30683/1929-2279.2025.14.24>

© 2025 Sivakumar and Thiyagarajan; Licensee Neoplasia Research.

This is an open-access article licensed under the terms of the Creative Commons Attribution License (<http://creativecommons.org/licenses/by/4.0/>), which permits unrestricted use, distribution, and reproduction in any medium, provided the work is properly cited.